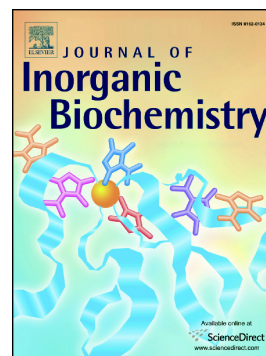


Journal Pre-proof

Coordination chemistry and catalytic applications of Pd(II)–, and Ni(II)–sulfosalan complexes in aqueous media

Norbert Lihi, Szilvia Bunda, Antal Udvardy, Ferenc Joó



PII: S0162-0134(19)30640-3

DOI: <https://doi.org/10.1016/j.jinorgbio.2019.110945>

Reference: JIB 110945

To appear in: *Journal of Inorganic Biochemistry*

Received date: 24 September 2019

Revised date: 18 November 2019

Accepted date: 20 November 2019

Please cite this article as: N. Lihi, S. Bunda, A. Udvardy, et al., Coordination chemistry and catalytic applications of Pd(II)–, and Ni(II)–sulfosalan complexes in aqueous media, *Journal of Inorganic Biochemistry* (2019), <https://doi.org/10.1016/j.jinorgbio.2019.110945>

This is a PDF file of an article that has undergone enhancements after acceptance, such as the addition of a cover page and metadata, and formatting for readability, but it is not yet the definitive version of record. This version will undergo additional copyediting, typesetting and review before it is published in its final form, but we are providing this version to give early visibility of the article. Please note that, during the production process, errors may be discovered which could affect the content, and all legal disclaimers that apply to the journal pertain.

© 2019 Published by Elsevier.

Coordination Chemistry and Catalytic Applications of Pd(II)–, and Ni(II)–Sulfosalan Complexes in Aqueous Media

Norbert Lihi,^{1*} Szilvia Bunda,^{2,3*} Antal Udvardy,² and Ferenc Joó^{1,2}

Affiliations

¹MTA-DE Redox and Homogeneous Catalytic Reaction Mechanisms Research Group,
Debrecen, Hungary

²University of Debrecen, Department of Physical Chemistry, Debrecen, Hungary

³University of Debrecen, Doctoral School of Chemistry

Mail

4002 Debrecen P.O.Box 400, Hungary

E-mail

lihi.norbert@science.unideb.hu

bunda.szilvia@science.unideb.hu

ABSTRACT

With the aim of identifying new types of water-soluble catalyst precursors for modification of biological membranes by homogeneous hydrogenation in aqueous solution and under mild conditions, we have performed detailed equilibrium and spectroscopic characterization of complex formation between nickel(II) or palladium(II) and salan-type ligands sulfonated in their aromatic rings (*N,N'*-bis(2-hydroxy-5-sulfonatobenzyl)-1,4-diaminoethane (HSS), *N,N'*-bis(2-hydroxy-5-sulfonatobenzyl)-1,4-diaminopropane (PrHSS) and *N,N'*-bis(2-hydroxy-5-sulfonatobenzyl)-1,4-diaminobutane (BuHSS)) in the slightly acidic – alkaline pH range. The stability constants of the metal complexes were determined using pH-potentiometry. The catalytic activities of the [Ni(HSS)] and [Pd(HSS)] complexes in hydrogenation and redox isomerization of oct-1-en-3-ol were also studied. The results indicate, that all of the investigated ligands exhibit excellent nickel(II) and palladium(II) binding ability *via* the formation of (O⁻,N,N,O⁻) linked chelate system. Both [Ni(HSS)] and [Pd(HSS)] catalyze the hydrogenation and redox isomerization of oct-1-en-3-ol. [Pd(HSS)] shows excellent activity and the reaction was highly selective to the formation of octan-3-ol. [Ni(HSS)] is also an active and selective catalyst for this hydrogenation reaction and to the best of our knowledge, [Ni(HSS)] is the first nickel(II)-based, hydrolytically stable, water-soluble catalyst bearing sulfonated salan moiety.

KEYWORDS

sulfonated salan, nickel(II), palladium(II), stability, hydrogenation, allylic alcohols

INTRODUCTION

Organometallic catalysis in aqueous media [1-5] have been widely used for studies on biological processes.[6] Such studies include modification of biological samples, both model systems (such as liposomes), isolated cell organelles, and live cells in order to gain insight on the role of biomembranes in various physiological processes.[6-8] Hyperpolarization of suitable biomolecules such as pyruvate *via* hydrogenation with para-H₂ is used for *in vivo* imaging. [9] In addition to other strict requirements (no toxicity!), the catalyst should be able to operate in aqueous environment, and solubility in water is often achieved by attaching polar or ionic substituents to the ligands of the catalytically active metal complex.

In addition to the studies on biochemistry or cell physiology, aqueous organometallic catalysis has also contributed very importantly to development of green chemical processes. Such processes facilitate reactions of environmentally important substrates (hydrogenation of carbon dioxide and various constituents of biomass) and also enable aqueous-organic liquid biphasic technologies. The latter are characterized by the use of a minimum amount of (or no) volatile organic solvents and by simple separation of products and catalysts, leading to highly efficient catalyst recycling and low metal contamination of the products. [2-4,8,10]

Salen (*N,N'*-ethylenebis(salicylimine)) is one of the most widely used ligands in coordination chemistry and its transition metal complexes show useful catalytic properties in non-aqueous media in reactions such as oxidation, hydrogenation, various C-C couplings, etc.). In order to capitalize on the versatile catalytic properties of salen complexes also in water, this ligand and its derivatives were made water-soluble by appending on it ionic or polar substituents such as, for example, sulfonate [11,12], carboxylate [13,14], ammonium [15], and phosphonium [16] groups. With respect to aqueous applications, however, a major drawback is in the imine character of the ligand, which often results in the hydrolysis and deterioration of the complexes in water especially under the sometimes harsh conditions of

catalysis (high temperature, presence of metal ions, bases or acids). [17] The problem of catalyst decomposition can be eliminated by hydrogenation of the C=N bonds leading to hydrolytically more stable complexes of *N,N'*-di(2-hydroxybenzyl)ethylenediamine (salan), or those of HSS = hydrogenated, sulfonated salen (Figure 1). [17,18] An excellent recent review discusses the synthesis and properties of salan complexes (both water-soluble and water-insoluble) as well as their biomedical and catalytic applications hitherto investigated. [19] Hydrogenation of salen-type ligands (e.g. those with various linker groups between the two salicylidene moieties) is – in principle – generally suitable also for the synthesis of hydrolytically stable sulfonated salan-type ligands (sulfosalans), however up till now this was only scarcely attempted. [10,19-21]

The use of water as solvent allows to carry out catalytic reactions at various pH which can be adjusted and controlled by addition of simple acids and bases (pH-static conditions are also used [22]). Variations in the pH of a reaction mixture may strongly influence the formation of various metal complex species (both their compositions and concentrations) and this may be reflected in the results of a catalytic reaction in terms of product(s) yield(s) and selectivities. [22] It is therefore important to learn the coordination chemistry of a given M^{n+}/L system even if the catalyst (or its precursor) is applied as a well-defined, isolated metal complex. For speciation studies in aqueous solutions, one of the most reliable and widely applicable methods is pH-potentiometry which may give information on the concentration distribution and the stoichiometry of the various metal complex species as the function of pH. On the basis of such speciations, it may be possible to identify the most abundant metal complex species under the conditions of catalysis (although this may not necessarily be identical to the real catalytic species).

((Please insert Figure 1 here))

In this paper, we report a detailed pH-potentiometric study of complex equilibria established in aqueous solutions of Pd^{2+} and Ni^{2+} complexes of three sulfosalan ligands (*N,N'*-bis(2-hydroxy-5-sulfonatobenzyl)-1,4-diaminoethane (HSS), *N,N'*-bis(2-hydroxy-5-sulfonatobenzyl)-1,4-diaminopropane (PrHSS) and *N,N'*-bis(2-hydroxy-5-sulfonatobenzyl)-1,4-diaminobutane (BuHSS), see Figure 1). Catalytic activities of the $[\text{Ni}(\text{HSS})]$ and $[\text{Pd}(\text{HSS})]$ complexes in hydrogenation and redox isomerization of oct-1-en-3-ol (as a representative allylic alcohol) are also reported.

EXPERIMENTAL

Synthesis and characterization of the sulfosalan ligands

HSS and BuHSS were prepared as described in [21] and were identified by their ^1H and ^{13}C NMR spectra, respectively. Synthesis of PrHSS was carried out analogously to the preparation of HSS and BuHSS; details of the synthesis and characterization (^1H , ^{13}C NMR and ESI-TOF MS data) can be found in the Supplementary. The precursor of PrHSS was prepared following the procedure described elsewhere. [23]

pH-potentiometry

$[\text{PdCl}_4]^{2-}$ stock solutions were prepared by dissolving $\text{Na}_2[\text{PdCl}_4]$ (Pressure Chemicals) in water using 2 equivalents of HCl to avoid hydrolytic processes. The NiCl_2 stock solution was prepared from the highest available grade and its concentration was checked gravimetrically. The purity and the concentration of the sulfosalan ligands and the concentration of $[\text{PdCl}_4]^{2-}$ stock solutions were checked by pH-potentiometry. For solution equilibrium studies, triple deionized and ultrafiltered (Milipore Q system) water was used.

The protonation constants of the HSS ligands (pK_a) and the overall stability constants of the metal complexes ($\log\beta_{pqrs}$) were determined by pH-potentiometric method. 15 mL aliquots of the ligands (ca. 2.1 mM concentration) were titrated with KOH solution of known concentration (ca. 0.16 M). The carbonate contamination (less than 0.1 %) and the concentration of the KOH solution were determined using the appropriate Gran functions. [24] During the titrations, the sample was purged with argon in order to ensure the absence of oxygen and carbon dioxide. The ionic strength of the samples was adjusted to 0.2 M KCl and the measurements were carried out at 298 K. The samples were stirred using a magnetic stirrer. The pH-potentiometric titrations were made using a computer-controlled Mettler Toledo T50 automatic titrator and the instrument was equipped with a DG 114-SC combined glass electrode (Mettler Toledo). The pH readings were converted to equilibrium hydrogen ion concentration as described by Irving et al. [25] The protonation constants and the overall stability constants of the metal complexes, $\beta_{pqrs} = [M_p L_q H_r Cl_s] / [M]^p [L]^q [H]^r [Cl]^s$ (where “M” stands for nickel(II) or palladium(II)) were calculated using the general computational programs (SUPERQUAD [26] and PSEQUAD [27]).

Spectroscopic measurements

^1H and ^{13}C NMR spectra were recorded in D_2O solutions on a Bruker Avance 360 spectrometer. When required, the pH of the samples was adjusted with the use of NaOD and DCl. ^1H and ^{13}C NMR chemical shifts are reported relative to DSS. ESI-TOF-MS (Electrospray Ionization Time-of-Flight Mass Spectrometry) measurements were carried out on a Bruker maXis II MicroTOF-Q instrument (Bruker Daltonik, Bremen, Germany) in negative ion mode. Details of the measurements can be found in the Supplementary.

UV-visible spectra of the nickel(II) complexes were recorded with an Agilent Technologies Cary 8454 UV-VIS diode array spectrophotometer in the 200 – 800 nm wavelength range using the same concentration range as in the pH-potentiometric titrations.

Typical procedure of hydrogenation and redox isomerization of oct-1-en-3-ol:

A solution of [Pd(HSS)] (1.25×10^{-7} to 2.5×10^{-7} mol) in water (100 – 200 μ L), oct-1-en-3-ol (2.5×10^{-4} mol), and 3 mL of 0.2 M acetate buffer of appropriate pH ($I=0.2$ M KCl) were placed into a high-pressure tube. The tube was repeatedly evacuated and filled with H₂ and finally pressurized with H₂ to reach 1 – 5 bar total pressure. The reaction vessel was immersed into a thermostated bath (25 – 80 °C), and the mixture was stirred for the desired reaction time. At room temperature the products were extracted with 2 mL of toluene, dried over MgSO₄, and subjected to gas chromatography.

In case of [Ni(HSS)] catalyst, the same procedure was used, however, the reaction mixture contained an aqueous solution of [Ni(HSS)] (1.07×10^{-5} mol in 1 mL of water), oct-1-en-3-ol (2.5×10^{-4} mol), and further 2 mL of water and the reactions were run at 80 °C.

The reaction mixtures were analyzed by gas chromatography using a HP5890 Series II equipment (Supelcowax 10 - Fused Silica 30 m \times 0.32 mm \times 0.25 μ m; FID; carrier gas: argon). Composition of the product mixtures are expressed as area %. The peaks in the chromatograms were identified by their order and standard samples and the composition of the product mixture was calculated from the peak areas.

RESULTS AND DISCUSSION

Acid-base properties of the ligands

The protonation constants (pK_a) of the ligands were determined by pH-potentiometric titrations and the data are collected in Table 1. The stepwise protonation constants of HSS

have already been published [17] and the two sets of data show excellent agreement. It follows from the structure of the investigated ligands, that in principle the sulfonic acid groups, the two phenolic-OH groups and the secondary amine groups may take part in deprotonation processes. However, the pH-potentiometric data clearly show, that the deprotonation of sulfonic acid groups takes place below $\text{pH} < 1.5$ which value falls out the potentiometrically measurable pH range. Therefore, four deprotonation constants have been determined by pH-potentiometry while the pH-dependent ^1H and ^{13}C NMR experiments offered a possibility to assign the pK_a values of the individual groups.

Table 1. Stepwise Deprotonation Constants (pK_a) of the Ligands^a

($I = 0.2 \text{ M KCl}$, $T = 298 \text{ K}$)

	HSS	PrHSS	BuHSS	BHBDPA ^{b,c}
H ₄ L	6.00(8)	6.93(8)	6.94(4)	5.90
H ₃ L	7.44(7)	7.82(8)	7.81(4)	8.47
H ₂ L	8.75(6)	9.57(7)	10.08(3)	10.16
HL	10.64(4)	11.28(4)	11.47(2)	11.13
$\Sigma\text{H}_i\text{L}$	32.83	35.60	36.30	35.66

^a 3σ standard deviations are in parentheses.

^b BHBDPA: (*N,N'*-bis(2-hydroxybenzyl)-2,3-diamino-propionic acid

^c Data are taken from Ref. [28]

Selected part of the proton decoupled ^{13}C NMR spectra of HSS as a function of pH are shown in Figure 2 and the chemical shifts of the carbon atoms as a function of pH are illustrated in the Supplementary, Figure S7. The $^{13}\text{C}\{^1\text{H}\}$ NMR spectra of the examined systems are available in the Supplementary (Figure S8, S9).

((Please insert Figure 2 here))

Based on the thorough analysis of NMR data it can be concluded, that the lowest, measurable pK_a value belongs to the deprotonation of one of secondary amino groups. In slightly acidic

pH range, a drastic downfield shift was observed in the aliphatic region of the NMR spectra confirming the aforementioned deprotonation process. This effect is well demonstrated in Figure S7, where the chemical shift of C8 carbon atom – assigned as one of the aliphatic carbon atoms – decreases by increasing the pH which corroborates that the deprotonation process occurs on the secondary amino group. The aromatic carbon atoms remain almost intact in this pH range. This, relatively low pK_a value for a secondary amine group, suggests the formation of an intramolecular hydrogen bond between the deprotonated amine and a protonated phenolic hydroxyl group.[28] A similar observation has already been reported in the case of (*N,N'*-bis(2-hydroxybenzyl)-2,3-diamino-propionic acid ligand (BHBDPA). [28] Upon increasing the pH, further deprotonation processes significantly overlap, however, based on the downfield shift in the aromatic part of the ^{13}C NMR spectra, these processes can be assigned to the deprotonation of phenolic hydroxyl groups, which can be easily followed on the chemical shift of C1 atom (Figure S7). In strongly alkaline solutions, the highest pK_a value belongs to the deprotonation of the other amine group resulting in further downfield shift in the aliphatic part of the ^{13}C NMR spectrum. The micro- and macroprocesses of HSS deprotonation are summarized in Scheme S1 (see Supplementary).

The results of pH-potentiometric measurements have also demonstrated, that the increasing size of the bridging unit between the two salicylamine moieties in PrHSS and BuHSS significantly enhances the basicity of the phenolic hydroxyl and the secondary amine groups resulting in higher basicity compared to that of HSS. This effect is also revealed by NMR spectroscopy where the downfield shift in the aliphatic region occurs in more alkaline pH for PrHSS and BuHSS than that obtained for HSS.

Pd(II) and Ni(II) complexes of the sulfosalan ligands

The equilibrium studies on the Pd(II)/Ni(II) – sulfosalan ligand systems were performed using pH-potentiometric titrations and the stability constants of the corresponding complexes are collected in Table 2. It is important to note, that chloride ion was used as a competitor during the titrations of Pd(II)/sulfosalan systems because the formation of $[\text{PdCl}_4]^{2-}$ and $[\text{PdCl}_3]^-$ species shifts the Pd(II)/sulfosalan complex formation into the measurable pH range. In the absence of chloride ion, the complexation occurs already under very acidic conditions hindering the determination of stability constants. [29]

Table 2. Stability Constants ($\log\beta_{pqrs}$) of the Complexes Formed between Palladium(II)^a or Nickel(II) and the Ligands^b ($I = 0.2 \text{ M KCl}$, $T = 298 \text{ K}$)

	HSS	PrHSS	BuHSS
[PdHLCl]	37.31(5)	36.98(6)	37.3(5)
[PdL]	31.2(2)	29.5(2)	31.7(5)
[NiLH]	18.7(1)	19.07(2)	15.98(5)
[NiL]	13.00(4)	12.15(2)	7.89(2)
pK_{PdL}^{PdHLCl}	6.11	7.48	5.60
pK_{NiL}^{NiHL}	5.70	6.92	8.09

^a Chloro complexes of palladium(II) were taken into account in the calculations of stability constants. These are as follows: $[\text{PdCl}]^+$ ($\log\beta = 5.08$); $[\text{PdCl}_2]$ ($\log\beta = 8.88$); $[\text{PdCl}_3]^-$ ($\log\beta = 11.30$); $[\text{PdCl}_4]^{2-}$ ($\log\beta = 12.18$). Data are taken from Ref. [30]

^b 3σ standard deviations are in parentheses.

As a representative example, the molar distribution of the complex species in the Pd(II):HSS 1:1 system are shown in Figure 3 while the distributions of the Pd(II):PrHSS 1:1 and the Pd(II):BuHSS 1:1 systems are reported in the Supplementary (Figure S10 and S11). In general, the complex formation processes with palladium(II) were quite fast; the titrations were performed in equilibrium controlled mode and the waiting time between two titration points fell into the range of 90 – 360 s.

For palladium(II), the complex formation in all cases starts with the ternary PdHLCl complex in slightly acidic pH range. In these complexes, the coordination sphere of Pd(II) is accommodated by the (O⁻,N,N) donor set and the square-planar environment is completed by

the binding of the chloride ion. Although the amino group is the most basic site in the ligands, the (O⁻,N,O⁻) coordination mode is unlikely. This can be explained by considering the fact, that the donor atoms in the ligands are in chelate position. Therefore, the coordination of the individual donors occurs in a cooperative manner. If the coordination mode is (O⁻,N,O⁻), a macrochelate complex forms in the PdHLCI species. With respect to thermodynamics, the formation of the coupled chelate system is more favourable than the formation of macrochelate species.

((Please insert Figure 3 here))

Upon increasing the pH, a further deprotonation process results in the formation of PdL complexes. In these complexes, the chloride ion is replaced by the phenolate O donor to form coupled chelate systems with ring sizes of (6,5,6), (6,6,6), and (6,7,6) in case of HSS, PrHSS, and BuHSS, respectively. Stability constants of the three PdL complexes are approximately the same, although Pd(II) prefers the (6,5,6) membered chelate systems. [31] This effect concerning the stabilities can be easily explained by considering the fact, that PrHSS and BuHSS have higher basicity than that of HSS resulting in increased stabilities. To compare the palladium(II) binding abilities of the sulfosalan ligands, theoretical distribution curves were calculated (Figure 4).

((Please insert Figure 4 here))

The calculated concentration distribution curves in a system containing Pd(II):HSS:PrHSS:BuHSS in 1:1:1:1 concentration ratio clearly demonstrate that HSS behaves as a more effective Pd(II) chelator than PrHSS or BuHSS. Under the conditions of Figure 4, HSS dominantly coordinates Pd(II) in the entire pH-range which is due to the formation of (6,5,6) membered chelate systems. Significant competition between HSS and

BuHSS occurs only in strongly alkaline pH-range, while only negligible complexation of Pd(II) by PrHSS is seen in the entire pH range; both effects are explained by the differences between the basicities of the studied sulfosalan ligands.

In general, palladium(II) forms more stable complexes than nickel(II) which is clearly shown by the stability constants in Table 2. For the nickel(II) – sulfosalan systems, the equilibrium features are the same than those of Pd(II) – sulfosalans, however, the stabilities and the amounts of the corresponding complexes are different. In all cases, the complex formation processes start with formation of an [NiHL] complex which, however, is only a minor species and its formation significantly overlaps with the formation of [NiL]. The distribution of the complexes formed in the Ni(II):HSS 1:1 system as a function of pH is shown in Figure 5. The coordination of an (O^- ,N,N, O^-) donor set results in the formation of square-planar complexes which is confirmed by UV-Vis spectroscopy. The coordination of nickel(II) to the ligands is accompanied by significant changes in the absorbance at 495 nm, which *d-d* band is characteristic for square-planar nickel(II) complexes. [32] The amount of the (O^- ,N,N, O^-) coordinated species reaches a maximum around at pH 8 confirming the equilibrium model obtained by pH-potentiometry in the Ni(II):HSS 1:1 system (Figure 6). The same tendencies were observed at 366 nm where the nickel(II)-phenolate MLCT band is characteristic. This corroborates that the NiHL complex features a (N,N, O^-) donor set which is completed by the binding of the phenolate group. In strongly alkaline solutions, there is no indication for the formation of mixed hydroxido species and the titration curves do not show any extra base consumption processes, thus these ligands are excellent chelators for nickel(II) and able to hinder the hydrolysis of the metal ion.

((Please insert Figure 5 here))

((Please insert Figure 6 here))

Comparison of the stability constants of NiL – sulfosalan complexes with HSS, PrHSS and BuHSS ligands, confirms that the (6,5,6)-membered chelate system is more favourable for nickel(II) than the (6,6,6)- or (6,7,6)-membered chelates; this results in high nickel binding ability (see Table 2; the theoretical species distributions are available in the Supplementary, Figure S12).

Catalytic applications of Pd(II)- and Ni(II)-sulfosalan complexes in hydrogenation/redox isomerization of allylic alcohols

Catalytic redox isomerization of allylic alcohols is a valuable, 100 % atom-economic synthetic process and various metal complexes are used as catalysts in this reaction. However, in most cases, such catalysts contain tertiary phosphine or *N*-heterocyclic carbene ligands [33-39], furthermore, application of Ni(II)-based catalysts for transposition of allylic alcohols is rare [40]. Pd(II)-complexes of HSS have already been applied successfully as catalysts in aqueous-phase hydrogenation and redox isomerization of allylic alcohols [20], as well as in Sonogashira [21] and Suzuki–Miyaura [10] C-C cross-coupling reactions. Isolated [Pd(HSS)] proved to be an active and selective catalyst for hydrogenation of α,β -unsaturated aldehydes (such as cinnamaldehyde). [41] More importantly for biological applications, [Pd(HSS)] could be effectively used for hydrogenation of phospholipids in aqueous dispersions (liposomes) and also for the hydrogenation of unsaturated fatty acyl residues in the bacterial cell membranes of *Pseudomonas putida* F1. [41] No such reactions were performed with Ni(II)-sulfosalan complexes. Furthermore, no attempt has been made to pinpoint the actual catalytic species in such reactions with the use of methods of coordination chemistry for identifying the possible species present in solution of the transition metal – sulfosalan (pre)catalysts. In aqueous organometallic catalysis, pH-potentiometry was conceived as a straightforward method to determine the various metal-sulfosalan species as a function of the

pH. Indeed, as described above, stability constants and molar distributions were determined for Pd(II)- and Ni(II)-complexes with HSS, PrHSS and BuHSS ligands.

The catalytic activity of [Ni(HSS)] was assessed in the reaction of oct-1-en-3-ol under H₂. In principle, the reaction can yield the hydrogenated product, octan-3-ol, and the product of redox isomerization octan-3-one (Scheme 1). These reactions were run at pH=7.04, where the [Ni(HSS)] species is far dominant and no free Ni(II) is present (Figure 5) – the pH of the reaction mixture did not change during the process. Under the conditions of Figure 7, the reaction proceeded smoothly and was highly selective for the formation of the saturated alcohol (C=C hydrogenation). It is remarkable that at a [substrate]/[catalyst] = 23.4 ratio, conversion of oct-1-ene-3-ol to octan-3-ol reached 80% in 3 h, which corresponds to a catalyst turnover frequency $\text{TOF} = 6.2 \text{ h}^{-1}$ ($\text{TOF} = \text{mol reacted substrate} \times (\text{mol catalyst} \times \text{time})^{-1}$). In comparison, under similar, albeit not identical conditions, the use of [Pd(HSS)] led to a $\text{TOF} = 650 \text{ h}^{-1}$. [20]

((Please insert Scheme 1 here))

((Please insert Figure 7 here))

The hydrogenation/redox isomerization of oct-1-en-3-ol catalyzed by [Ni(HSS)] was strongly influenced by the hydrogen pressure. As it is shown in Figure 8, there was only a 5 % conversion at $P(\text{H}_2) = 1 \text{ bar}$, which steadily increased with the pressure to reach 86 % at $P(\text{H}_2) = 5 \text{ bar}$.

((Please insert Figure 8 here))

These observations demonstrate, that [Ni(HSS)] is an active and selective catalyst for the hydrogenation of the C=C double bond in allylic alcohols with no significant selectivity towards formation of saturated ketones. According to the species distribution curve (Figure

5), at the pH = 7.04 of aqueous solutions of the [Ni(HSS)] catalyst, the dominant species is [NiL]²⁻ albeit minor amounts of [NiHL]⁻ are also present. It should be considered, though, that the species distribution was calculated for $T = 25.0$ °C and $I = 0.2$ M (KCl) and it should not be taken directly relevant for the reaction conditions. Clearly, further detailed studies are needed to close the gap between the conditions of equilibrium and kinetic studies. Nevertheless, [Ni(HSS)] is reported here as the first nickel(II)-based, hydrolytically stable, water-soluble catalyst containing a sulfonated salan ligand, which – due to its significant catalytic activity in hydrogenation of allylic alcohols – deserves further scrutiny.

In aqueous solutions, [Pd(HSS)] catalyzed the hydrogenation /redox isomerization of oct-1-en-3-ol with excellent activity (TOF up to 1894 h⁻¹ at 40 °C), and the reaction was highly selective to the formation of octan-3-ol (maximum yield 85.6 %). It is important to note, that in separate experiments under the conditions of Figure 9, there was no hydrogenation of octan-3-one to octan-3-ol, meaning that the reaction involves hydrogenation of the C=C bond in oct-1-en-3-ol and the redox isomerization followed by C=O hydrogenation route can be excluded.

The reaction was run at several pH, and the results are shown in Figure 9. It was found, that raising the pH from 3.6 to 4.6 resulted in a drop of the conversion of oct-1-en-3-ol from 36.5 % to 11.0 %, however, further increase of the pH led to a steep increase of the conversion reaching 94.7 % at pH 8.2. The molar distribution of the complexes formed in the Pd(II): HSS 1:1 system as a function of pH is shown in Figure 3. It can be seen that at 25.0 °C, the dominant species both at pH 3.6 and 4.6 is [PdHLC1]²⁻ which is gradually replaced by [PdL]²⁻ upon increasing the pH up to 8.2. This leads to the conclusion, that in this system the catalytically most active species is [PdL]²⁻, and that the hydrogenation of oct-1-en-3-ol at pH 4.2 and below may be due to [PdL]²⁻ which is present in about 10 % at pH 4.2, and/or to the ternary chlorido complexes which can be found in small but not negligible

concentrations at pH 3.6. It should be emphasized here, too, that the conditions of the equilibrium (speciation) studies and those of the catalytic measurements were not exactly the same, although in these investigations 0.2 M KCl was applied in all measurements and the difference of the temperatures used for equilibrium and catalytic experiments was only 15 °C.

CONCLUSIONS

In summary, with the use of pH potentiometry, we have determined the protonation constants of three sulfonated salan ligands, HSS, PrHSS, and BuHSS, as well as the equilibrium constants for the stepwise formation of their complexes with Pd²⁺ and Ni²⁺. In a parallel study we determined the catalytic activity of [Ni(HSS)] and [Pd(HSS)] complexes in the hydrogenation and redox isomerization of oct-1-en-3-ol which revealed significant activity also in the case of the non-precious metal complex [NiL]²⁻. The catalytic activity of [Pd(HSS)] was also determined as a function of the pH. Comparison of the pH-dependence of the catalytic activity to the species distribution determined by pH-potentiometry led to the conclusion that [PdL]²⁻ possesses the highest catalytic activity in this reaction.

Although this approach may help in identifying actual catalytic species in homogeneous catalysis in aqueous solutions, nevertheless, the results should be evaluated with due care, especially when there is a considerable gap between the experimental conditions of speciation and catalytic studies.

ABBREVIATIONS

HSS	<i>N,N'</i> -bis(2-hydroxy-5-sulfonatobenzyl)-1,4-diaminoethane
PrHSS	<i>N,N'</i> -bis(2-hydroxy-5-sulfonatobenzyl)-1,4-diaminopropane
BuHSS	<i>N,N'</i> -bis(2-hydroxy-5-sulfonatobenzyl)-1,4-diaminobutane

DSS	Sodium trimethylsilylpropanesulfonate
MLCT	Metal to Ligand Charge Transfer
TOF	Turnover Frequency

ACKNOWLEDGEMENTS

The research was supported by the EU and co-financed by the European Regional Development Fund (under the projects GINOP-2.3.2-15-2016-00008 and GINOP-2.3.3-15-2016-00004). N. L., A. U. and F. J. are grateful for the financial support of the Hungarian National Research, Development and Innovation Office (NKFIH PD-128326 and FK-128333). This work was also supported by ÚNKP-19-3 New National Excellence Program of the Ministry for Innovation and Technology.

REFERENCES

- [1] F. Joó, *Aqueous Organometallic Catalysis*, Kluwer, Dordrecht, 2001.
- [2] B. Cornils, W. A. Herrmann (Eds.), *Aqueous-Phase Organometallic Catalysis. Concepts and Applications*, 2nd edn., Wiley-VCH, Weinheim, 2004.
- [3] D. J. Adams, P. J. Dyson, S. J. Tavener, *Chemistry in Alternative Reaction Media*, Wiley, Chichester, 2004.
- [4] P. Dixneuf, V. Cadierno (Eds.), *Metal-Catalyzed Reactions in Water*, Wiley-VCH, Weinheim, 2013.
- [5] L.-A. Schaper, S. J. Hock, W. A. Herrmann, F. E. Kühn, *Angew. Chem. Int. Ed.* 52 (2013) 270–289; *Angew. Chem.* 125 (2013) 284–304.
- [6] I. Horváth, A. Glatz, V. Varvasovszki, Zs. Török, T. Páli, G. Balogh, E. Kovács, L. Nádasdi, S. Benkő, F. Joó, L. Vígh, *Proc. Natl. Acad. Sci. USA* 95 (1998) 3513–3518.
- [7] P.J. Quinn, F. Joó, L. Vígh, *Prog. Biophys. Mol. Biol.* 53 (1989) 71–103.

- [8] F. Joó, *Acc. Chem. Res.* 35 (2002) 738–745.
- [9] G. Papp, H. Horváth, F. Joó, *ChemCatChem* 11 (2019) 3000–3003.
- [10] Sz. Bunda, A. Udvardy, K. Voronova, F. Joó, *J. Org. Chem.* 83 (2018) 15486–15492.
- [11] Y.-S. Liu, N.-N. Gu, P. Liu, X.-W. Ma, Y. Liu, J.-W. Xie, B. Dai, *Tetrahedron* 71 (2015) 7985–7989.
- [12] S. Noël, F. Perez, J. T. Pedersen, B. Alies, S. Ladeira, S. Sayen, E. Guillon, E. Gras, C. Hureau, *J. Inorg. Biochem.* 117 (2012) 322–325.
- [13] J. C. Pessoa, S. Marcão, I. Correia, G. Gonçalves, Á. Dörnyei, T. Kiss, T. Jakusch, I. Tomaz, M. M. C. A. Castro, C. F. G. C. Geraldes, F. Avecilla, *Eur. J. Inorg. Chem.* (2006) 3595–3606.
- [14] S. A. Samokhvalova, V. A. Ershov, D. A. Lukyanov, P. S. Vlasov, O. V. Levin, *Russ. J. Gen. Chem.* 89 (2019) 852–855.
- [15] Y. A. Rulev, Z. Gugkaeva, V. I. Maleev, M. North, Y. N. Belokon, *Beilstein J. Org. Chem.* 11 (2015) 1614–1623.
- [16] M. N. Dehkordi, A.-K. Bordbar, P. Lincoln, V. Mirkhani, *Spectrochim. Acta A* 90 (2012) 50–54.
- [17] I. Correia, J. C. Pessoa, M. T. Duarte, M. F. M. da Piedade, T. Jakusch, T. Kiss, M. M. C. A. Castro, C. F. G. C. Geraldes, F. Avecilla, *Eur. J. Inorg. Chem.* (2005) 732–744.
- [18] I. Correia, Á. Dörnyei, T. Jakusch, F. Avecilla, T. Kiss, J. C. Pessoa, *Eur. J. Inorg. Chem.* (2006) 2819–2830.
- [19] J. C. Pessoa, I. Correia, *Coord. Chem. Rev.* 388 (2019) 227–247.
- [20] K. Voronova, M. Purgel, A. Udvardy, A. C. Bényei, Á. Kathó, F. Joó, *Organometallics* 32 (2013) 4391–4401.
- [21] K. Voronova, L. Homolya, A. Udvardy, A. C. Bényei, F. Joó, *ChemSusChem* 7 (2014) 2230–2239.

- [22] F. Joó, J. Kovács, A. C. Bényei, Á. Kathó, *Angew. Chem. Int. Ed.* 37 (1998) 969–970; *Angew. Chem.* 110 (1998) 1024–1026.
- [23] H. Diehl, C. C. Hach, *Inorg. Synth.* 3 (1950) 196–201.
- [24] G. Gran, *Analyst* 77 (1952) 661–671.
- [25] H. M. Irving, M. G. Miles, L. D. Pettit, *Anal. Chim. Acta* 38 (1967) 475–488.
- [26] P. Gans, A. Sabatini, A. Vacca, *J. Chem. Soc. Dalton* (1985) 1195–1200.
- [27] L. Zékány, I. Nagypál in: D. Leggett (Ed.), *Computational Methods for the Determination of Formation Constants*, Plenum Press, New York, 1985, pp. 291–353.
- [28] A. Jancsó, Z. Paksi, S. Mikkola, A. Rockenbauer, T. Gajda, *J. Inorg. Biochem.* 99 (2005) 1480–1489.
- [29] N. Lihi, D. Sanna, I. Bányai, K. Várnagy, I. Sóvágó, *New J. Chem.* 41 (2017) 1372–1379.
- [30] L. I. Elding, *Inorg. Chim. Acta* 7 (1973) 581–588.
- [31] L. Cattalini, A. Cassol, G. Marangoni, G. Rizzardi, E. Rotondo, *Inorg. Chim. Acta*, 3 (1969) 681–684.
- [32] G. Sciortino, N. Lihi, T. Czine, J.-D. Maréchal, A. Lledós, E. Garribba, *Int. J. Quant. Chem.* 118 (2018) e25655.
- [33] R. Uma, C. Crévisy, R. Grée, *Chem. Rev.* 103 (2003) 27–51.
- [34] V. Cadierno, P. Crochet, J. Gimeno, *Synlett* (2008) 1105–1124.
- [35] V. Cadierno, P. Crochet, J. Francos, S. E. García-Garrido, J. Gimeno, N. Nebra, *Green. Chem.* 11 (2009) 1992–2000.
- [36] F. Scalambra, P. Lorenzo-Luis, I. de los Rios, A. Romerosa, *Coord. Chem. Rev.* 313 (2019) 118–148.
- [37] P. Lorenzo-Luis, A. Romerosa, M. Serrano-Ruiz, *ACS Catalysis* 2 (2012) 1079–1086.
- [38] F. Scalambra, M. Serrano-Ruiz, A. Romerosa, *Dalton Trans.* 46 (2017) 5864–5871.

- [39] J. Francos, S. E. García-Garrido, J. García-Álvarez, P. Crochet, J. Gimeno, V. Cadierno, *Inorg. Chim. Acta* 455 (2017) 398–414.
- [40] H. Bricout, E. Monflier, J.-F. Carpentier, A. Mortreux, *Eur. J. Inorg. Chem.* (1998) 1739–1744.
- [41] R. Gombos, B. Nagyházi, F. Joó, *React. Kinet. Mech. Cat.* 126 (2018) 439–451.

Journal Pre-proof

Figure 1. Sulfonated tetrahydrosalen (sulfosalan) ligands used in this study.

Figure 2. Selected part of the ^{13}C NMR spectra of HSS as a function of pH. $c_{\text{HSS}} = 10 \text{ mM}$.

Figure 3. The distribution of the complexes formed in the Pd(II):HSS 1:1 system as a function of pH, $c_{\text{L}} = 2.0 \text{ mM}$.

Figure 4. Theoretical distribution curves calculated in the Pd(II):HSS:PrHSS:BuHSS 1:1:1:1 system at $c_{\text{L}} = 2.0 \text{ mM}$.

Figure 5. Distribution of the complexes formed in the Ni(II):HSS 1:1 system and the absorbance values obtained by UV-Vis spectroscopy at 366 nm as a function of pH. $c_{\text{L}} = 2.0 \text{ mM}$

Figure 6. Selected UV-Vis spectra in the Ni(II):HSS system at 1:1 metal to ligand ratio as a function of pH. $c_{\text{L}} = 2.0 \text{ mM}$

Figure 7. Time course of the hydrogenation and redox isomerization of oct-1-en-3-ol catalyzed by [Ni(HSS)] (\blacktriangle – oct-1-en-3-ol, \blacksquare – octan-3-ol, \bullet – octan-3-one). Conditions: $n([\text{Ni}(\text{HSS})]) = 1.07 \times 10^{-5} \text{ mol}$, $n(\text{oct-1-en-3-ol}) = 2.5 \times 10^{-4} \text{ mol}$, 3 mL water, $p\text{H} = 7.04$, $P(\text{H}_2) = 5 \text{ bar}$, $T = 80 \text{ }^\circ\text{C}$.

Figure 8. The effect of hydrogen pressure on the hydrogenation and redox isomerization of oct-1-en-3-ol catalyzed by [Ni(HSS)] (\blacktriangle – oct-1-en-3-ol, \blacksquare – octan-3-ol, \bullet – octan-3-one). Conditions: $n([\text{Ni}(\text{HSS})]) = 1.07 \times 10^{-5} \text{ mol}$, $n(\text{oct-1-en-3-ol}) = 2.5 \times 10^{-4} \text{ mol}$, 3 mL water, $p\text{H} = 7.04$, $t = 3 \text{ h}$, $T = 80 \text{ }^\circ\text{C}$.

Figure 9. Conversion of oct-1-en-3-ol (\blacklozenge) and yields of octan-3-ol (\blacksquare) and octan-3-one (\bullet) in hydrogenation and redox isomerization of oct-1-en-3-ol catalyzed by [Pd(HSS)] as a function of pH. Conditions: $n([\text{Pd}(\text{HSS})]) = 2.5 \times 10^{-7} \text{ mol}$, $n(\text{oct-1-en-3-ol}) = 2.5 \times 10^{-4} \text{ mol}$, 3 mL acetate buffer, $I = 0.2 \text{ M KCl}$, $P(\text{H}_2) = 1 \text{ bar}$, $t = 30 \text{ min}$, $T = 40 \text{ }^\circ\text{C}$.

Scheme 1. Hydrogenation and redox isomerization of oct-1-en-3-ol catalyzed by [Ni(HSS)].

Declaration of interests

The authors declare that they have no known competing financial interests or personal relationships that could have appeared to influence the work reported in this paper.

Journal Pre-proof

Graphical abstract

Formation constants of nickel(II) and palladium(II) complexes of sulfonated salan ligands were determined by pH-potentiometric titrations. In addition to hydrogenation of unsaturated lipids in model and biomembranes, these water-soluble, selective catalysts proved outstandingly effective for the hydrogenation and redox isomerization of oct-1-en-3-ol, too.

Journal Pre-proof

HIGHLIGHTS

- Organometallic catalysis in aqueous media to study biological processes
- Sulfonated salan-type ligands are excellent water-soluble metal chelators
- Homogeneous catalysis in aqueous media with Pd(II)- and Ni(II)-sulfosalan complexes
- High activity and selectivity in hydrogenation and redox isomerization

Journal Pre-proof

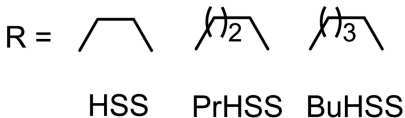
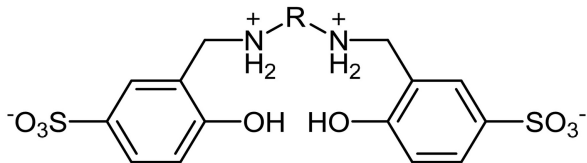


Figure 1

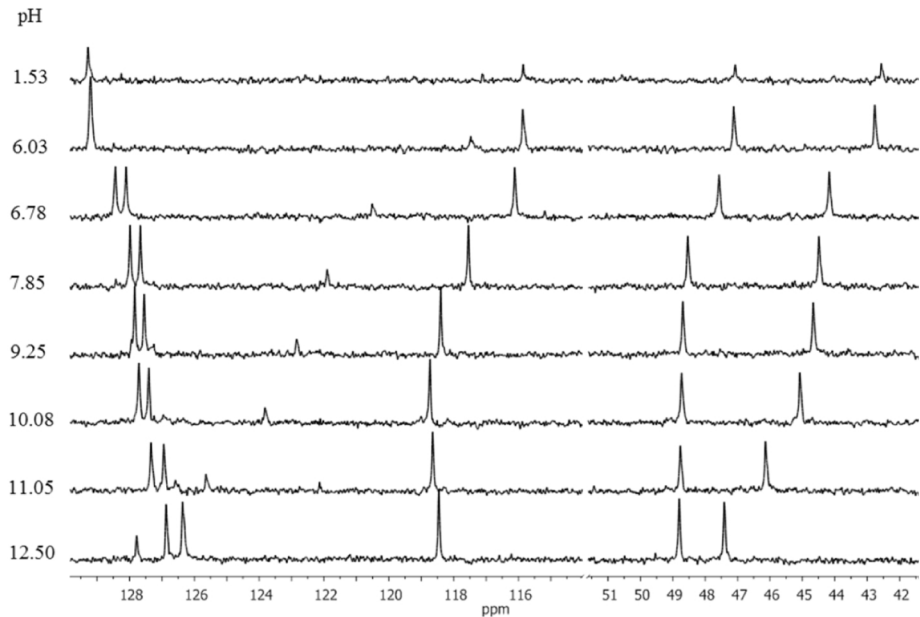


Figure 2

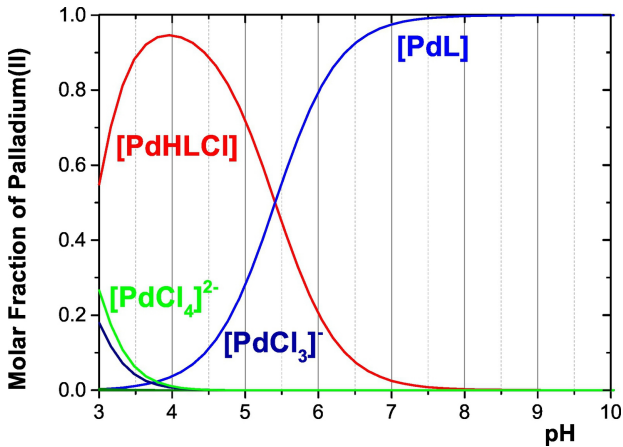


Figure 3

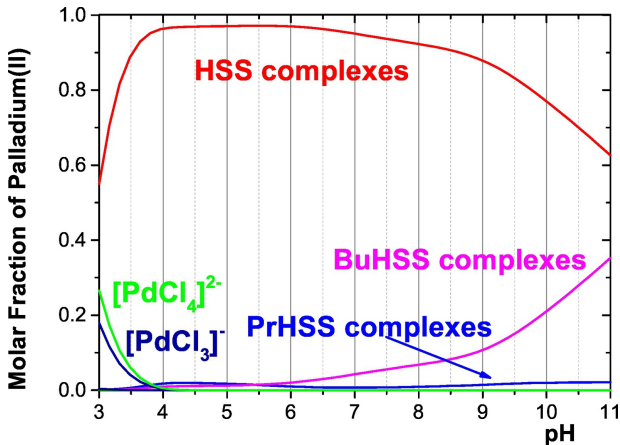


Figure 4

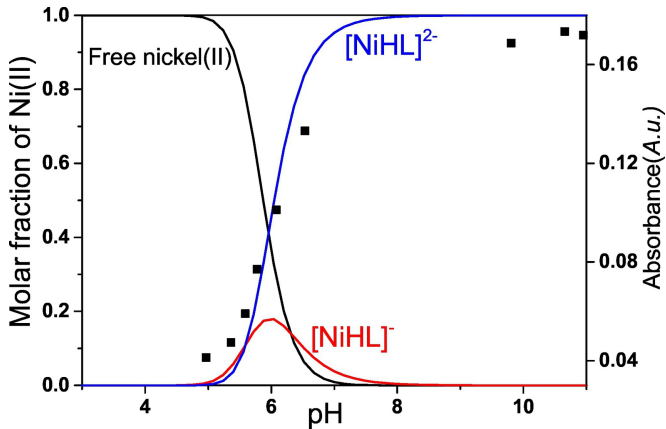


Figure 5

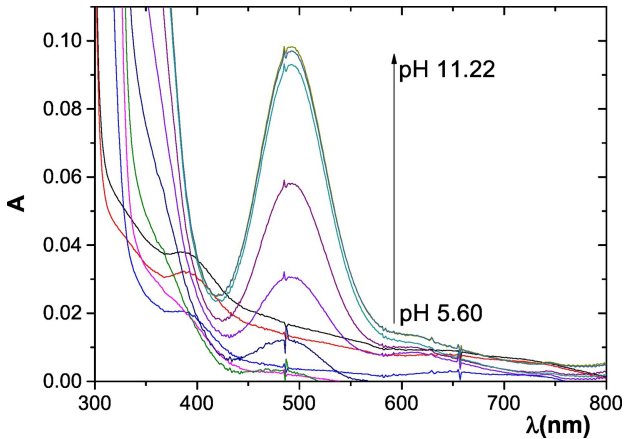


Figure 6

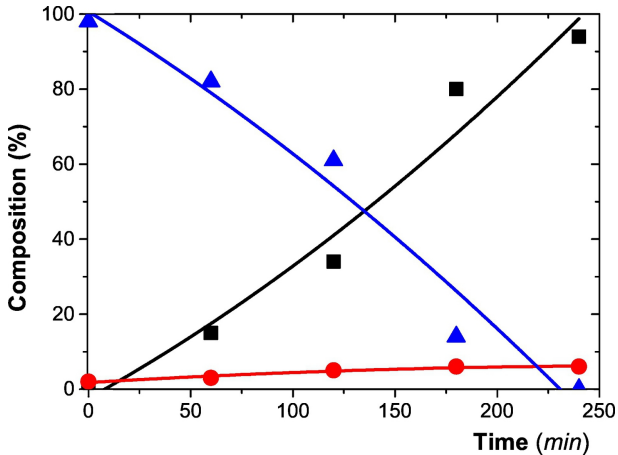


Figure 7

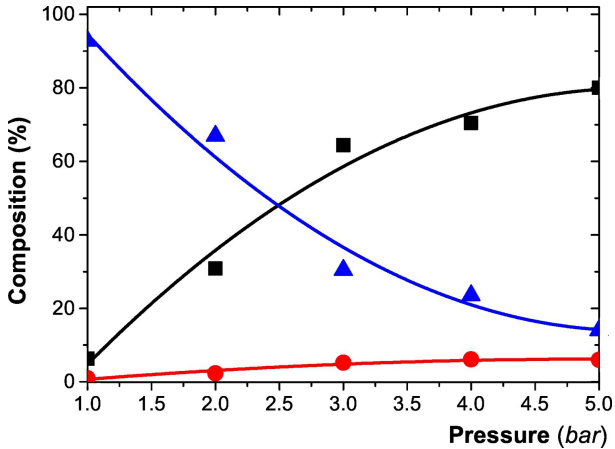


Figure 8

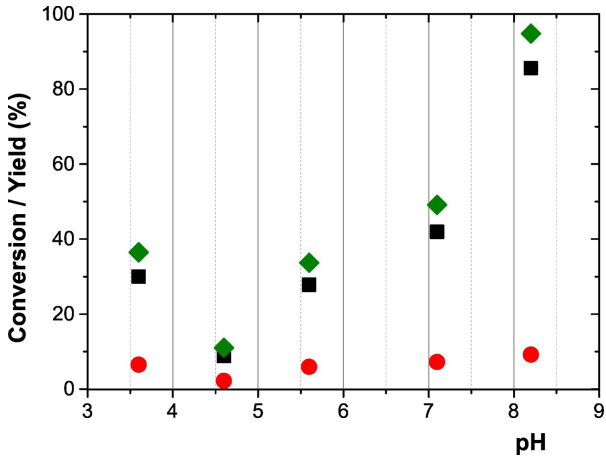


Figure 9

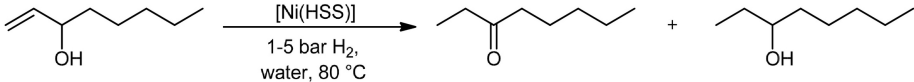


Figure 10